J. Physiol. (1984), **349**, *pp.* 205–226
With 2 plates and 12 text-figures
Printed in Great Britain

ELECTROPHYSIOLOGICAL PROPERTIES OF GUINEA-PIG THALAMIC NEURONES: AN *IN VITRO* STUDY

BY HENRIK JAHNSEN* AND RODOLFO LLINÁS

From the Department of Physiology & Biophysics, New York University Medical Center, 550 First Avenue, New York, NY 10016, U.S.A.

(*Received 1 June 1983*)

SUMMARY

1. The electroresponsive properties of guinea-pig thalamic neurones were studied using an *in vitro* slice preparation.

2. A total of 650 cells were recorded intracellularly comprising all regions of the thalamus; of these 229 fulfilled our criterion for recording stability and were used as the data base for this report. The resting membrane potential for thirty-four representative neurones which were analysed in detail was -64 ± 5 mV (mean $\pm$ S.D.), input resistance 42 ± 18 MΩ, and action potential amplitude 80 ± 7 mV.

3. Intracellular staining with horseradish peroxidase and Lucifer Yellow revealed that the recorded cells had different morphology. In some their axonal trajectory characterized them as thalamo-cortical relay cells.

4. Two main types of neuronal firing were observed. From a membrane potential negative to -60 mV, anti- or orthodromic and direct activation generated a single burst of spikes, consisting of a low-threshold spike (l.t.s.) of low amplitude and a set of fast superimposed spikes. Tonic repetitive firing was observed if the neurones were activated from a more positive membrane potential; this was a constant finding in all but two of the cells which fulfilled the stability criteria.

5. The l.t.s. response was totally inactivated at membrane potentials positive to -55 mV. As the membrane was hyperpolarized from this level the amplitude of the l.t.s. increased and became fully developed at potentials negative to -70 mV. This increase is due to a de-inactivation of the ionic conductance generating this response. After activation the l.t.s. showed refractoriness for approximately 170 ms. De-inactivation of l.t.s. is a voltage- and time-dependent process; full de-inactivation after a step hyperpolarization to maximal l.t.s. amplitude (-75 to -80 mV) requires 150–180 ms.

6. Membrane depolarization positive to -55 mV generated sudden sustained depolarizing 'plateau potentials', capable of supporting repetitive firing (each action potential being followed by a marked after-hyperpolarization, a.h.p.). The a.h.p. and the plateau potential controlled the voltage trajectory during the interspike interval and, with the fast spike, constitute a functional state where the thalamic neurone displayed oscillatory properties.

* Present address: Institute of Neurophysiology, Blegdamsvej 3C, DK-2200 Copenhagen N, Denmark.

7. Frequency–current (*f–I*) plots from different initial levels of membrane potential were obtained by the application of square current pulses of long duration (2 s). From resting membrane potential and from hyperpolarized levels a rather stereotyped onset firing rate was observed due to the presence of the l.t.s. After this initial response, the firing was modulated by the amplitude of the stimulus. At membrane potentials positive to −55 mV, the firing frequency was always directly modulated by the amplitude of the current pulse.

8. We conclude that neurones in different parts of the thalamus have similar electrophysiological properties, that they are capable of burst firing and tonic firing, and that, in addition, they can display self-supporting oscillatory states.

INTRODUCTION

The electrophysiological properties of neurones which constitute the thalamic nuclei have been the subject of much research over the last three decades (for a general review of thalamic function, see Shepherd, 1979). It is nevertheless only recently that the necessary techniques have been developed to determine directly the electrophysiological properties of these cells under circumstances allowing direct control of the ionic environment as well as other physical and chemical parameters. In this paper and the one that follows, we describe experiments which relate to the electrophysiological properties of the different cellular groups in the guinea-pig thalamus and the ionic requirements necessary for their generation. At the beginning of the study, we expected that the functional properties of these cells would vary among the thalamic nuclei. Having recorded from neurones in all major nuclear groups, we conclude that thalamic cells behave more as a single population than anticipated, given the diversity of their inputs and the variety in their individual morphology.

In this first paper, the electrophysiological properties of the cells will be explored using intracellular recording techniques. In the accompanying report, the ionic behaviour and some of the pharmacological aspects of the conductances which generate these electrophysiological properties will be analysed in detail. Some of the material presented in these papers has been published as preliminary reports (Llinás & Jahnsen, 1982; Jahnsen & Llinás, 1982).

METHODS

The techniques utilized in this set of experiments are very similar to those described in previous papers from this laboratory (Llinás & Sugimori, 1980).

Tissue preparation. Thalamic slices were obtained from albino guinea-pigs 8–15 weeks old, weighing 275–500 g. Animals were anaesthetized with ether and decapitated. The dorsal part of the cranium was removed to expose the forebrain and cerebellum. Using a spatula, the brain was rapidly lifted from the cranial base and the rostral and caudal ends of the brain were transected in order to isolate the diencephalic mass containing the thalamic nuclei. At this point the diencephalon was dissected free *en bloc* from the surrounding tissue.

Slices of the diencephalon were obtained in either the coronal, parasagittal or horizontal plane (Pl. 1), depending on the particular nuclei to be studied and the manner in which the neuronal afferents were to be stimulated. The 400 μm-thick slices were obtained by using an Oxford G501 vibratome after the tissue was cemented to the bottom of a Plexiglas chamber and supported by agar blocks to prevent deformation during cutting. All of the above steps, except for the cementing procedure, were performed under standard Ringer solution at 6–10 °C.

Once sectioned, the slices were incubated for at least an hour at room temperature in vials filled with oxygenated saline solution. During the experiment the slices were transferred one at a time to the recording chamber where they were continually superfused with oxygenated saline, maintained at 37 °C with a feed-back temperature control system. Since the recording chamber and solutions utilized are the same as those described previously (Llinás & Sugimori, 1980), we will not duplicate that description here. One of the main differences between cerebellar slices and those obtained from the thalamus relates to visualization of the cells. Cerebellar slices reveal clearly the anatomical organization of the cellular elements; by contrast, in thalamic slices only the outlines of the different nuclei can be recognized. Indeed single elements could rarely be seen and thus penetration was performed blindly with regard to particular neuronal elements. Although this is a serious limitation in determining the exact location of a recording electrode within a given neurone (e.g. soma *vs.* dendrite), the location of particular cells with respect to the main subdivisions of the thalamic nuclei was generally quite unambiguous.

Recording and staining. The intracellular records in these studies were obtained using K^+-acetate-filled micro-electrodes with an input resistance of 60–120 MΩ. The neurones were activated directly through the recording electrode by means of a boot-strap amplifier circuit. Anti- or orthodromic stimulation was obtained using a twisted wire pair located near the mid line or in the white matter at different points on the periphery of the thalamic nuclear mass. The morphology of the recorded neurones was directly demonstrated by means of intracellular injection of horseradish peroxidase or Lucifer Yellow following the procedures outlined in previous papers (Llinás & Sugimori, 1980).

RESULTS

Distribution of the recorded thalamic neurones

The data base for these two papers consists of 650 cells of which 229 were held for sufficient time to determine their electrophysiological properties under optimum conditions. By this we mean a stable recording maintained for at least 10 min with a resting potential no smaller than −55 mV, and input resistance and time constant of at least 15 MΩ and 5 ms respectively. Often neurones could be recorded for periods of up to 4 h. In most of the recordings the electrode was actively withdrawn at the end of the recording in order to verify the value of the resting potential initially recorded. Thus while close to two-thirds of the cells recorded did not meet our optimum recording requirements, the results obtained from these transient recordings did corroborate, without exception, the electrophysiological properties observed in the remaining 229 cells selected according to the above criteria.

The anatomical distribution of the cells in this group is indicated in Fig. 1 as dots in a rostral–caudal coronal reconstruction of the thalamus based on the stereotaxic atlases of Tindal (1965) and Luparello (1967). Since the precise demarcation of the thalamic subnuclei is somewhat arbitrary, we clustered them into seven major groups (Pl. 1). These were the anterior group (anterodorsal, anteromedial and anteroventral nuclei), the medial group (central, medial, paraventricular, paracentral, parataenial, reuniens and rhomboid nuclei), the ventral group (ventro-dorso-medial, ventro-lateral and ventral-medial nuclei), the posteromedial group (parafascicular nucleus and nucleus of posterior commissure), the posterior group (pretectal and posterior nuclei), the lateral nucleus and the lateral geniculate nucleus. We recorded from 6 cells in the anterior group, 123 medial, 32 ventral, 21 posteromedial and 4 posterior. Recordings were also obtained from 18 neurones in the lateral nucleus and 21 in the lateral geniculate nucleus. Although the medial geniculate nucleus was not included in our reconstruction in Fig. 1, recordings from four cells in this nucleus indicate that

the properties of these cells are identical to those from the other parts of the thalamus. Short-term recordings were also obtained from three cells in the nucleus reticularis. Two were close to the ventral group of nuclei and the third deeper in the nucleus. Although none of these three last recordings met our standard of 10 min recording stability, the electrophysiology was similar to that of the rest of the neurones studied.

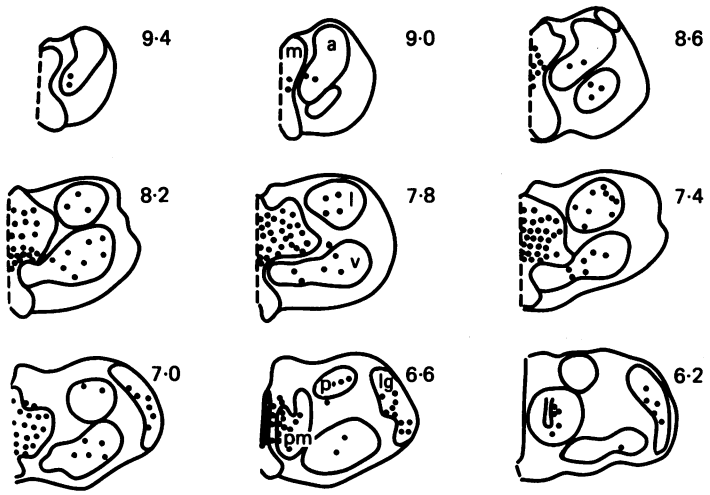

Fig. 1. Location of 225 thalamic neurones from which stable, long-term, intracellular recordings were obtained. The recordings were from both right and left sides of the diencephalon, but for the sake of simplicity all the cells are shown on the same side. The sections are coronal reconstructions based on the stereotaxic atlases of Tindal (1965) and Luparello (1967). Numbers correspond to distance in millimetres anterior to the interaural plane. Abbreviations: a, anterior group; l, lateral group; lg, lateral geniculate; m, medial group; p. posterior group; pm, posteromedial group; and v, ventral group.

The morphological observations, based on fifty neurones intracellularly marked with horseradish peroxidase or Lucifer Yellow injection (as shown in Pl. 2), correspond to the anatomical descriptions obtained from Golgi material in related rodents as well as in other mammalian forms (Ramón y Cajal, 1911; Guillery, 1966; Scheibel & Scheibel, 1966; Grossman, Lieberman & Webster, 1973; Friedlander, Lin, Stanford & Sherman, 1981). At least some of the cells were thalamocortical relay cells since axons from stained cells in fortunate sections could be seen leaving the thalamus in the direction of the cerebral cortex.

Electrophysiological results

The present results were obtained by intracellular recording from neurones in all of the main thalamic nuclear subdivisions. From our total data base the electrophysiological properties of only two neurones (described at the end of the paper) deviated from the following description.

TABLE 1. Values for resting potential (V_{rest}), spike height (V_{spike}), rate of rise and input resistance for thirty-four representative neurones for five different nuclear groups

Location	V_{rest} (mV)	V_{spike} (mV)	Rate of rise (V/s)	Input resistance (MΩ)
Posterolateral group	62	76	173	56
	61	74	225	20
	60	88	182	43
	62	81	262	20
	65	76	193	70
	64	74	230	17
	72	81	291	23
Medial group	66	88	264	66
	67	82	193	73
	72	80	240	33
	72	95	227	58
	66	76	242	43
	71	91	245	45
	71	81	289	61
	61	76	144	40
Ventral group	65	76	187	55
	70	86	274	36
	61	76	210	17
	62	82	240	63
	65	91	262	26
	61	87	248	44
	62	76	141	42
	62	77	239	20
	61	81	254	42
Lateral group	56	68	140	56
	59	77	310	30
	56	74	198	68
	59	77	284	34
	64	81	225	22
	63	85	304	25
	74	91	209	26
Anterior group	68	82	172	36
	60	81	175	46
	55	65	182	75
$n = 34$	64·0 ± 5·0	80·4 ± 6·6	225·1 ± 46·7	41·8 ± 18·2

All values are mean ± S.D., and the cells in each group are consecutive recordings.

Resting potential

Table 1 gives the values for thirty-four randomly selected neurones. Their resting potential was found to vary between −55 (our cut-off criterion) and −74 mV with a mean of −64 and a standard deviation of 5 mV ($n = 34$). The mean input resistance, determined by intracellular injection of small-amplitude current pulses (0·1–0·2 nA), was 42 MΩ (S.D. = 18, $n = 34$) and the mean time constant 14 ms (S.D. = 6, $n = 34$). These values agreed closely with the rest of the recorded cells.

Direct stimulation

The basic electrophysiological characteristics of thalamic neurones become patently clear when short outward current pulses are delivered to the cell. A typical example of the responses observed is illustrated in Fig. 2. If a depolarizing pulse, subthreshold at resting membrane potential (Fig. 2*B*), was repeated during a small d.c. depolarization (*C*) or hyperpolarization (*A*) of the cell, two quite distinct responses were

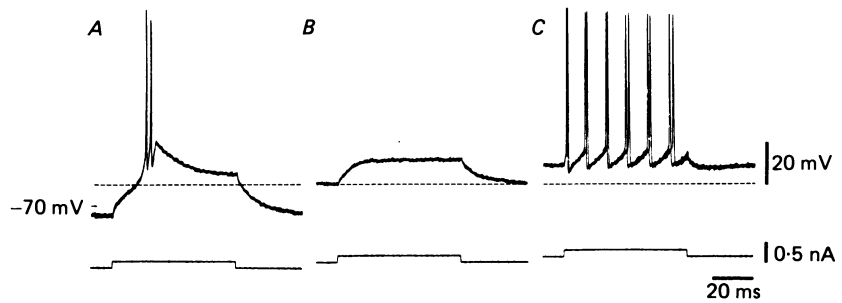

Fig. 2. Stimulation of thalamic cell with a constant amplitude transmembrane current pulse at three different membrane potentials. In this and the following Figures the resting potential of the cell is given in mV and its level indicated to the left with an arrow. In *A* the cell was directly stimulated while being hyperpolarized by a constant current injection. The outward current pulse triggers an all-or-none burst of spikes. In *B* the same current pulse produces a subthreshold depolarization if superimposed on a slightly depolarized membrane potential level. In *C*, after further depolarization by a direct current, the current pulse produce a train of action potentials. Dashed line serves as a reference level which indicates a low excitability point between *A* and *C*. Note the different firing levels in records *A* and *C*.

observed. If the neurone was depolarized (Fig. 2*C*), the previously subthreshold depolarizing pulse generated a train of action potentials, each followed by a clear after-hyperpolarization. If, on the other hand, the same subthreshold depolarizing pulse was delivered following a slight d.c. hyperpolarization (Fig. 2*A*), a singular burst of action potentials was generated. This latter response had an abrupt onset and was crowned by one or several fast action potentials, after which the membrane potential returned to near passive potential level.

Antidromic invasion

The basic phenomenology observed following direct stimulation could also be seen following either antidromic or orthodromic activation. Indeed, as shown in Fig. 3*A–C*, antidromic invasion of thalamic cells following white-matter stimulation produced different responses depending on the initial membrane potential. At rest (−60 mV, *B*), antidromic invasion of these cells was characterized by a short-lasting action potential (1·0–1·2 ms) which often demonstrated an initial segment–soma dendritic break of its rising phase and a fast falling phase followed by a prolonged after-depolarization. The prolonged after-depolarization was produced, in part, by a voltage-dependent conductance which at this level of membrane potential cannot be fully activated (see below).

If the cell was depolarized by 14 mV, to −46 mV, before antidromic activation

(Fig. 3*A*), the antidromic potential showed a decrease in amplitude and a marked after-hyperpolarization which could last for as long as 100 ms. Upon hyperpolarization by 10 mV from rest (Fig. 3*C*), white-matter stimulation generated, following the initial antidromic spike, the after-depolarization observed in Fig. 3*B* but in addition, because this after-depolarization was increased in amplitude and duration, a burst

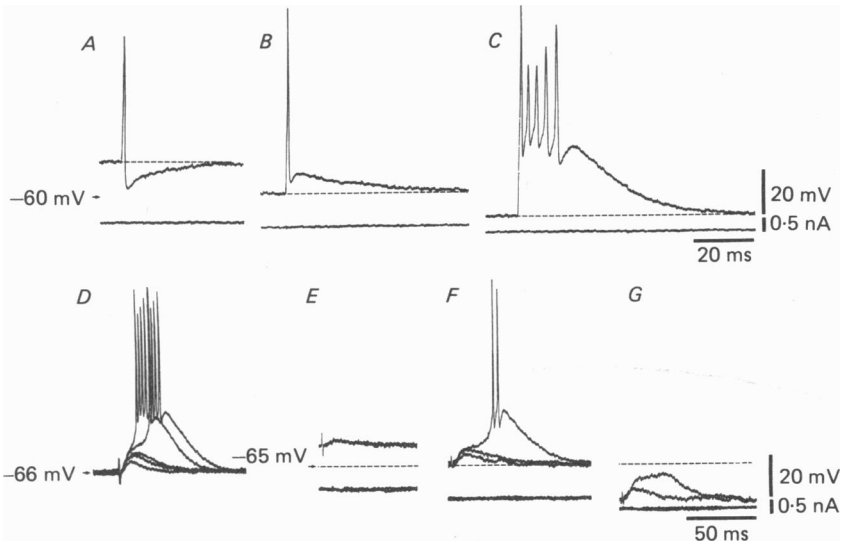

Fig. 3. Antidromic and orthodromic activation following bipolar stimulation in the mid line. *A*, *B* and *C*, antidromic invasion of a neurone at three different membrane potentials. At a depolarized level (*A*) the stimulation produced a fast spike followed by a marked after-hyperpolarization. At approximately −60 mV (*B*) the fast antidromic spike is followed by an after-depolarization most likely caused by activation of a Ca^{2+} conductance not fully de-inactivated at this level. At the hyperpolarized level (*C*) the antidromic spike was followed by a typical burst response. *D*, orthodromic activation of increasing intensity produced e.p.s.p.s of increasing amplitude. The largest e.p.s.p.s reached threshold for the burst response. *E*, *F* and *G*, synaptic activation at three different membrane potentials in another cell. At the depolarized level the e.p.s.p. did not reach the threshold for the fast spike (*E*). At rest (*F*), e.p.s.p.s reached the threshold for the burst response de-inactivated at this level whereas at the hyperpolarized level the e.p.s.p.s produced only the l.t.s.

of spikes resembling those observed following direct stimulation from a hyperpolarized level (Figs. 2*A* and 4*C*). When fully developed this burst activation was often characterized by one to seven fast action potentials of which the first was the largest. The spikes that followed immediately were smaller but increased in amplitude later in the burst.

Synaptic inputs

Both excitatory and inhibitory synaptic activations were observed in this preparation (see Methods). Synaptic activation could produce a burst of spikes directly from resting potential if this potential was more negative than −65 mV. In Fig. 3*D*, graded synaptic potentials were shown to generate an all-or-none burst of spikes

whose latency was dependent on the amplitude of the synaptic input. This latter point is clearly seen in the records shown in Fig. 3*E–G* in another cell. Here d.c. modulation of the membrane potential level could transform the burst generated by a synaptic potential at rest to a synaptic depolarization incapable of firing the cell (Fig. 3*E* at −55 mV) to one capable of generating only a graded response which does not reach threshold for the activation of the fast spikes (Fig. 3*G* at −82 mV).

At normal resting level, inhibitory synaptic potentials were rarely observed. They became quite clear when the membrane potential was slightly depolarized, indicating that $E_{\text{i.p.s.p.}}$ (driving force for i.p.s.p.) was too close to resting potential to generate a significant driving force. Also spontaneous unitary inhibitory synaptic potentials were occasionally recorded under these latter conditions.

Local synaptic interaction

In order to determine whether electrical or chemical local synaptic interactions occur between thalamic cells, fourteen pairs of cells separated by no more than 250 μm, were simultaneously recorded. In no case did spike activity in any of the cells produce post-synaptic potentials in the second cell; furthermore, no sign of electrical coupling between cells was ever recorded. Similarly, none of the thirty neurones that were stained with Lucifer Yellow were dyecoupled to any other cells in the slice. However, because of the relatively small number of double recordings, local synaptic interactions cannot be totally ruled out in this preparation (cf. Ralston, 1979).

General characteristics of low-threshold spike response

As demonstrated above, thalamic neurone spike bursts could be generated by relatively small depolarizations when the resting membrane potential was negative to −65 mV. The burst was characterized by its all-or-none nature, and its amplitude was related to the membrane potential before generation. It had a stereotyped wave form for a given initial membrane potential level and a sufficient time interval (more than 170 ms) between pulses. The burst response was composed of two distinct parts, (i) the low threshold spike proper (l.t.s.): a slowly rising and falling triangle-like potential which had a rather low threshold firing level, and (ii) a rapid succession of fast spikes which occurred most generally at the crest of the slower l.t.s. and which reached firing level at approximately −40 mV resting potential. These two components will be shown in the accompanying report (Jahnsen & Llinás, 1984) to be generated by different ionic conductances.

Electrophysiological properties of the l.t.s. If a depolarizing square pulse, subthreshold at rest, was superimposed on different levels of hyperpolarization, the first phenomenon observed was the appearance of a low-amplitude, slow-rising, all-or-none depolarization (Fig. 4*A* and *B*). As the stimulus was superimposed on more negative membrane potential levels, this response had a faster onset and larger amplitude and reached the firing level for the fast action potentials (Fig. 4*C*). A similar set of findings could be obtained as rebound post-anodal exaltations following hyperpolarizing pulses of different amplitude (Fig. 4*D* and *E*). Note that for small hyperpolarizations the rebound response was small and had a very slow rate of rise. As the hyperpolarization was increased, the rebound component (shown at higher gain in *E*)

became higher in amplitude and faster in its rate of rise without affecting the over-all duration. When the rebound response became large enough, a fast action potential was generated.

De-inactivation of the l.t.s. by membrane hyperpolarization. The relation between the initial membrane potential and the amplitude and rate of rise of the l.t.s. is illustrated

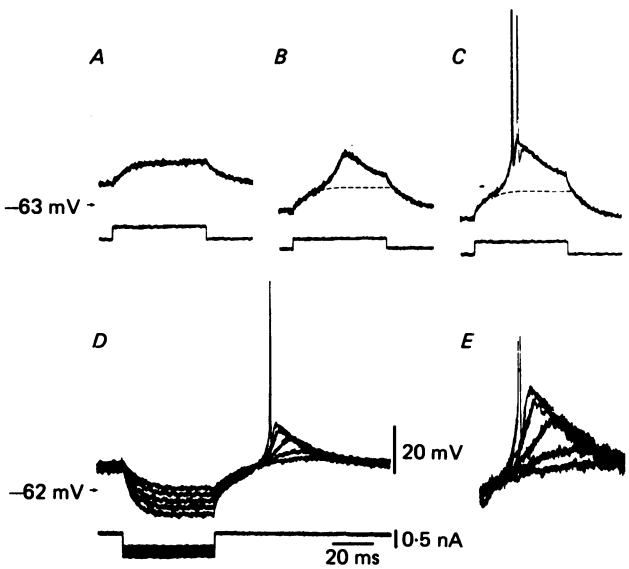

Fig. 4. The two components of the burst response: the l.t.s. and the fast spike component. *A*, *B* and *C*, constant amplitude depolarizing current pulses superimposed on three different levels of membrane potential. In *A* the pulse is a subthreshold depolarization. Hyperpolarization produces a slowly rising all-or-none l.t.s. (*B*) and finally the full-blown burst response consisting of a slow depolarization and fast spikes (*C*). *D*, hyperpolarizing current pulses of increasing amplitude caused a rebound burst response at the current break. As the amplitude of the pulses was increased, the rebound slow depolarization increased in size and rate of rise until a fully developed burst response was seen as a post-anodal exaltation. At higher gain (*E*) the graded nature of the post-anodal response becomes visible as the membrane potential is released from different levels of hyperpolarization.

in Fig. 5. In Fig. 5*A* two l.t.s.s (lower records) were generated from two different resting levels by a threshold current pulse of fixed amplitude after blockage of the fast spike by tetrodotoxin (TTX) (see accompanying paper). The recording to the left was obtained from −60 mV, that to the right from −70 mV.

These l.t.s.s are characterized by a rate of rise and amplitude which is dependent on the initial value of the resting potential. Their rising phase was in all cases faster than the falling phase and in general the duration fluctuated, from cell to cell, between 20 and 30 ms. The upper traces in Fig. 5*A* show a first derivative of the action potential, shown immediately underneath, after subtracting the passive component of the response. Note the clear difference in the rate of rise given by the voltage derivative of this spike at these two membrane levels. The amplitude of the voltage derivative was plotted against membrane potential in Fig. 5*B*. The plot indicates that

the l.t.s. was absent below −55 mV, where the voltage-dependent conductance generating the spike was totally inactivated. From this level the rate of rise of the l.t.s. increased and reached a maximum at −70 mV beyond which level its amplitude remained constant. This de-inactivation plot is in fact very similar to that previously published for the inferior olive neurones (Llinás & Yarom, 1981*b*, Fig. 3), the threshold for the l.t.s. being only slightly modified by the initial membrane potential as demonstrated in the plot in Fig. 5*C*.

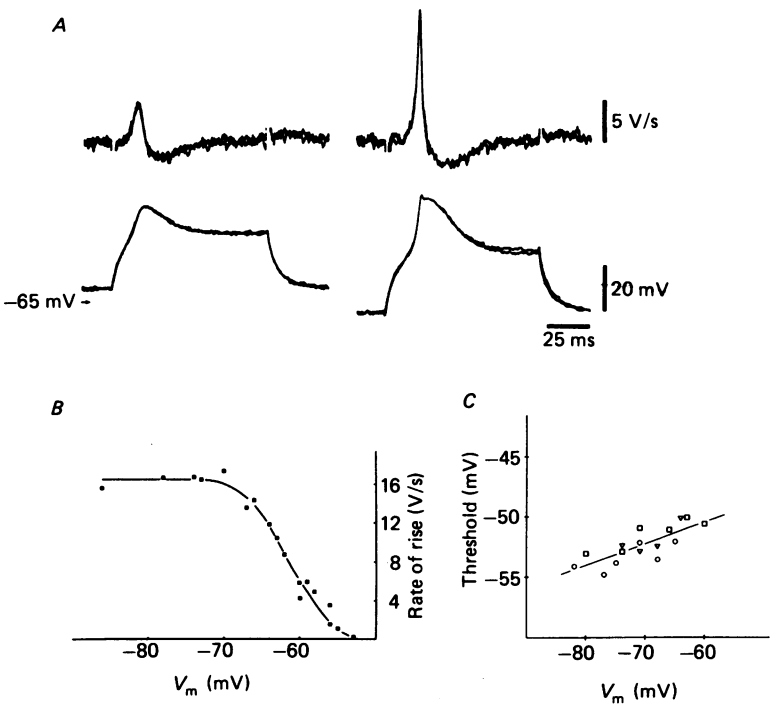

Fig. 5. Voltage dependency of l.t.s. de-inactivation. *A*, depolarizing current pulses from different holding potentials produced a l.t.s. of different amplitude (lower traces) following TTX addition to the bath. Differentiation of these responses (after subtraction of the passive component of the depolarization) gives an estimate of the rate of rise of the l.t.s. from different membrane potentials (upper traces). Assuming that the l.t.s. is proportional to the rate of rise of the spike, it was possible to make an estimate of the de-inactivation of the l.t.s. conductance by plotting the rate of rise against the holding potential as shown in *B*. It shows that the conductance is fully inactivated at potentials positive to −55 mV and completely de-inactivated at values negative to −70 mV. *C*, threshold for l.t.s. as a function of initial membrane potential shown for three different cells under standard conditions.

Time dependence of the l.t.s. de-inactivation. The above de-inactivation was not only voltage- but also time-dependent. Thus, if the membrane potential was abruptly hyperpolarized from a level of complete inactivation to a level sufficient to allow l.t.s. activation, a minimum time at the hyperpolarized membrane level was required before de-inactivation. This is shown in Fig. 6*A*, where the response of a cell to a test depolarizing pulse was determined at different times after the onset of a

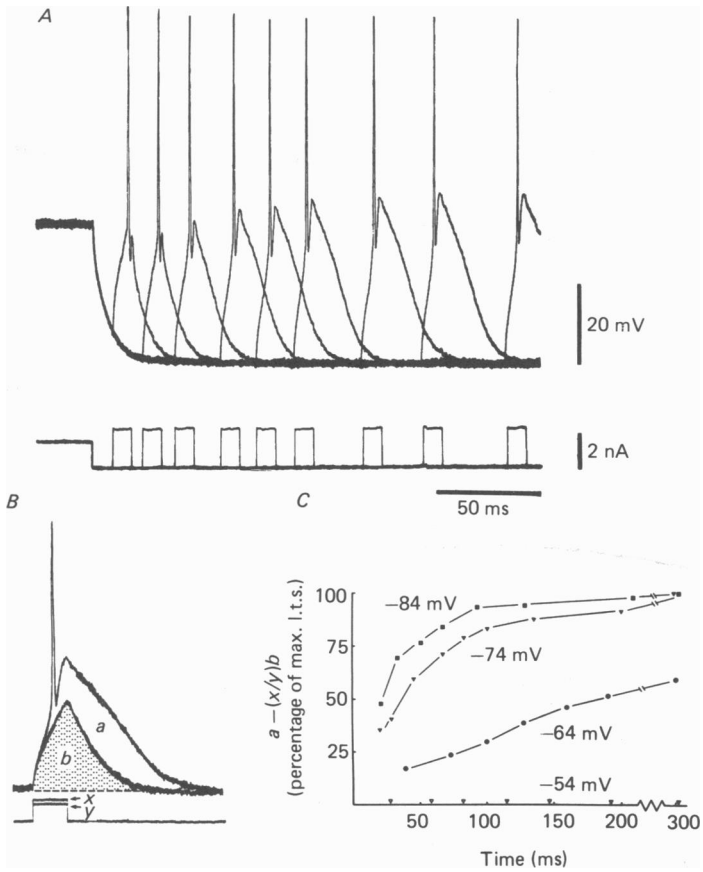

Fig. 6. De-inactivation of the burst response. In *A* a neurone was depolarized with a direct current to about −44 mV. A hyperpolarization of 30 mV was then produced with a long-lasting current pulse. At different times during the hyperpolarization the response of the membrane was tested by injection of a depolarizing pulse. Nine such tests at different intervals are superimposed. The response of the membrane increased in amplitude and duration as the interval increased. *B*, difference between a subthreshold depolarization (*b*) and an l.t.s. (*a*). The de-inactivation of the l.t.s. plotted in *C* was calculated as $a-(x/y)b$ where a is the area under the l.t.s., b the area under the subthreshold response, and x and y the amplitude of the corresponding current pulses. *C*, demonstration that the de-inactivation is both a time- and voltage-dependent process. The results of four experiments are similar to those shown in *A* are plotted. The cell was hyperpolarized from −44 mV to −54, −64, −74 and −84 mV. Full de-inactivation was only obtained for hyperpolarizations to −74 and −84 mV. No de-inactivation was seen at −54 mV.

hyperpolarizing step to −74 mV from an initial holding potential of −44 mV. The illustration shows that the l.t.s. increased in amplitude and duration as the interval between the onset of membrane hyperpolarization and the test pulse increased. A measurement of the increased l.t.s. response with time was calculated by measuring the area of the l.t.s. (*a* in Fig. 6*B*) and subtracting from it a just-subthreshold depolarization (*b*). This latter value was multiplied by a small correcting factor (x/y) to compensate for the increased value of a due to the larger current injection. The

increase in l.t.s. was plotted as a function of membrane potential for four different hyperpolarizing step amplitudes. It demonstrates that the de-inactivation time was dependent on the level of conditioning hyperpolarization and that the time required to reach over 90% de-inactivation was 150–180 ms for hyperpolarizations more negative than −80 mV. Note that in this plot −74 and −84 mV hyperpolarizations were capable of producing maximum l.t.s. However, at −64 mV membrane potential the de-inactivation reached only 50% of the maximum and this was not achieved until 300 ms.

Refractoriness of the l.t.s. All of the electrophysiological characteristics explored to this point for the l.t.s. indicate that it is generated by a conductance which is inactive at potentials more positive than −55 mV and which, as in the inferior olive (Llinás & Yarom, 1981*b*), is de-inactivated by hyperpolarization. This being the case, the l.t.s. should demonstrate refractoriness to the generation of a second response even at a maintained hyperpolarized membrane level. This refractory period is shown in Fig. 7*A*, which illustrates that following an initial l.t.s. a second current injection, although larger than the test pulse, activated only the fast action potential. The transition between refractory period and the complete burst is shown in the plot, indicating that a full recovery of the bursting response occurred after 170 ms, in keeping with similar measurements in other neurones in the study.

Plateau potential and after-hyperpolarization response

A rather different phenomenology from that recorded following a hyperpolarizing potential could be observed if thalamic neurones were depolarized from rest. Often when the membrane potential was near −55 mV a small d.c. step of less than 0·1 nA triggered an abrupt change in membrane potential which lasted for the duration of current flow (Fig. 8*A*). This response reached a peak and was maintained as a plateau potential. Short outward current pulses superimposed on this plateau potential could activate all-or-none fast spikes followed by a prolonged after-hyperpolarization (a.h.p.) (Fig. 8*A–C*). Often, either following a single short stimulus or spontaneously, the neurone reached a level such that it maintained an oscillatory firing as a steady functional state (Fig. 8). This plateau potential is similar to that found in the Purkinje cells (Llinás & Sugimori, 1980). Its ionic basis will be discussed in the accompanying paper (Jahnsen & Llinás, 1984).

Thalamic cells are capable of generating a very marked a.h.p., especially when activated on the plateau potential as shown in Fig. 8*A*. In the case illustrated in Fig. 8*B*, the neurone was directly activated by a train of very short depolarizing pulses superimposed on a d.c. polarization which held the membrane potential at −47 mV. The a.h.p.s generated under these conditions had a large constant amplitude and a long duration which was often potentiated with repeated activation. The a.h.p. resembled a large inhibitory post-synaptic potential (i.p.s.p.) but was actually produced by the activation of a K^+ conductance (some of which was voltage-dependent and some Ca^{2+}-dependent) and by the slow re-activation of the plateau potential, as described above. This last point is particularly clear in part *C* of Fig. 8 where the fast action potentials were superimposed and the a.h.p. demonstrated a concave trajectory and a small voltage rebound, similar to that observed at the beginning of the d.c. pulse.

A different approach was used to study the time course of the membrane potential between spikes; specifically, the time course with which the membrane potential returned to base line following a hyperpolarizing current pulse was investigated (Fig. 9*A*). Here the cell was artificially depolarized to −45 mV by a direct current injection and from this initial value the potential was abruptly moved to −85 mV by an inward

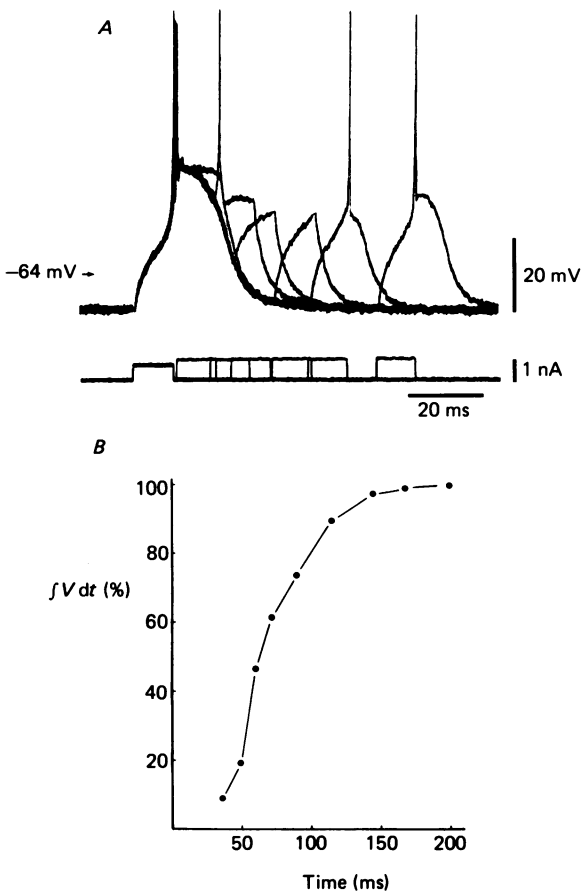

Fig. 7. *A*, refractory period of the l.t.s. Following an initial l.t.s., injection of test current pulses demonstrates refractoriness for the generation of a second l.t.s. even though the test pulse is larger than the conditioning pulse (*A*). *B* plots the size of the test response (measured as the integral of the voltage as a percentage of the initial response) against the interval.

current pulse. At the break of this pulse, the membrane potential demonstrated a rather slow concave return to base line. This slow return was accelerated as the membrane potential reached firing level for the rebound response. As shown in the accompanying paper (Jahnsen & Llinás, 1984), this slow return to base line was generated by the activation of an early K^+ current (I_A) similar to that described by Hagiwara, Kusano & Saito (1961) and by Connor & Stevens (1971) and encountered

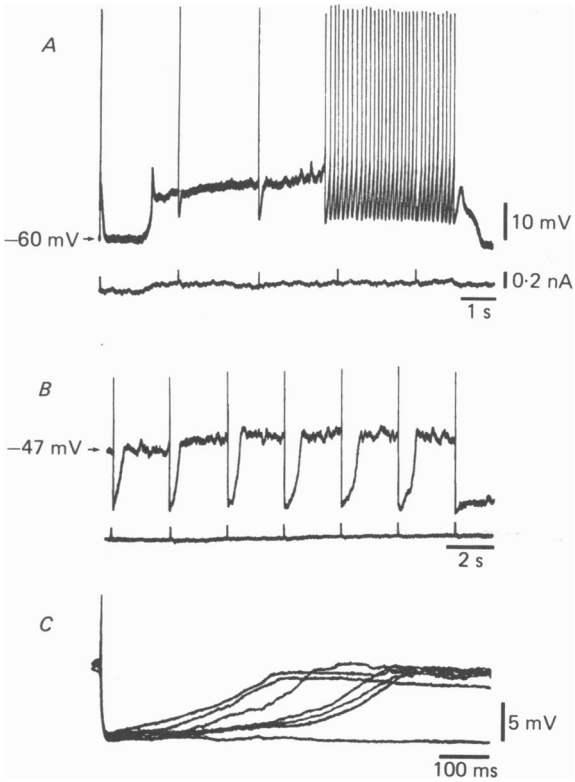

Fig. 8. The plateau depolarization and the after-hyperpolarization. *A*, injection of a minute constant current produced approximately a 12 mV depolarization with an initial overshoot probably caused by the l.t.s. Although the current was not increased during the first 4 s of the plateau depolarization, the cell depolarized an additional 4 mV. Then a slight increase in the current led to repetitive firing. When the current injection was terminated at the end of the sweep, the potential returned to its initial level. *B*, after-hyperpolarization (a.h.p.) following brief intracellular stimulation. The membrane potential was held at a depolarized level with a bias current. Each stimulus was followed by an action potential (not shown in full) and an a.h.p. In this cell the a.h.p. increased in duration during repetitive activation. *C*, the seven a.h.p.s. shown in *A* were superimposed. The membrane potential indicated to the left in *B* is not the resting value which in this cell was well below −60 mV.

in the C.N.S. in cells such as the vagal motoneurone (Yarom, Sugimori & Llinás, 1980) and in hippocampal neurones (Gustafsson, Galvan, Grafe & Wigström, 1982). By contrast, if the hyperpolarizing pulse was generated from a level closer to rest, the membrane potential was seen to return to base line rapidly without demonstrating this K^+ conductance change. The time dependence for the de-inactivation of this A current is illustrated on the right (Fig. 9*B*).

In short then, from a membrane potential positive to about −55 mV, the early K^+ conductance inactivated. If the cell was hyperpolarized for a minimum period (more than 6 ms), this K^+ conductance became de-inactivated and was then activated if a sufficient depolarization occurred from this new level. Once activated, the

conductance prevented an immediate return of the potential to base line for up to 100 ms, after which time it became inactive once again. The role of this I_A component in the oscillatory properties of thalamic neurones will be discussed in the accompanying paper (Jahnsen & Llinás, 1984).

Finally, the possibility must be considered that the a.h.p. may involve some measure of recurrent inhibition. Such inhibition could be induced, in principle, by

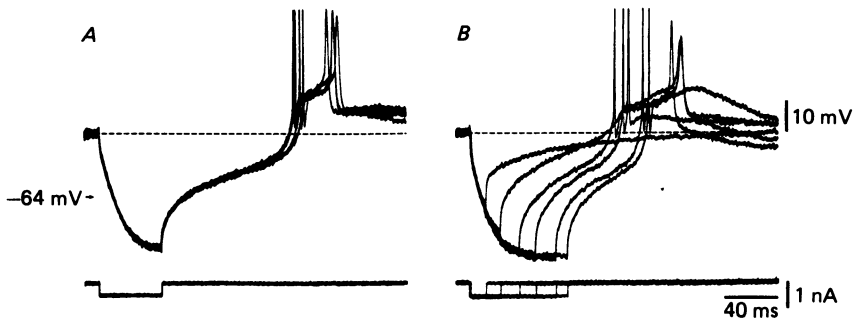

Fig. 9. Delayed return of membrane potential after injection of hyperpolarizing pulse. The cell was depolarized to about −45 mV with a constant current injection. In *A* the membrane was hyperpolarized to −85 mV. At the break of the current pulse the potential did not immediately return to base line but showed a concave trajectory. The hyperpolarization eventually resulted in a rebound burst (the amplitude of the fast spikes is truncated). In *B* change in the duration of the hyperpolarization demonstrates the time dependence for both the a.h.p. and the l.t.s.

the activation of axon collaterals of thalamic neurones (Andersen & Sears, 1964) or by recurrent inhibition involving dendrodendritic reciprocal synapses (Famiglietti & Peters, 1972; Spaćek & Lieberman, 1974). Although the possibility is remote, given the all-or-none nature of the a.h.p. and its K^+-dependence, in four experiments γ-aminobutyric acid antagonists such as bicucculine and picrotoxin in concentrations up to 300 μM were applied to the bath in order further to test this possibility. In all such experiments no variation in the duration or amplitude of the a.h.p. was observed, suggesting absence of any inhibitory component. On the other hand, the potentiation of a.h.p.s with repetitive activation must be related to either a potentiation of the Ca^{2+}-dependent K^+conductance or to the recruitment of further Ca^{2+} entry, probably at dendritic sites (see accompanying paper).

Repetitive firing and frequency–current relations (f–I)

Several unusual properties of the repetitive firing of thalamic neurones were investigated. If the membrane potential was maintained depolarized by a prolonged current pulse applied from a potential negative to −70 mV, both the burst and the tonic responses fused to generate a continuous repetitive discharge (Fig. 10). However, the initial firing rate was always dominated by the presence of the l.t.s. which produces a burst of spikes. During the post-burst period the action potentials re-established a more or less constant amplitude and duration as the current injection proceeded.

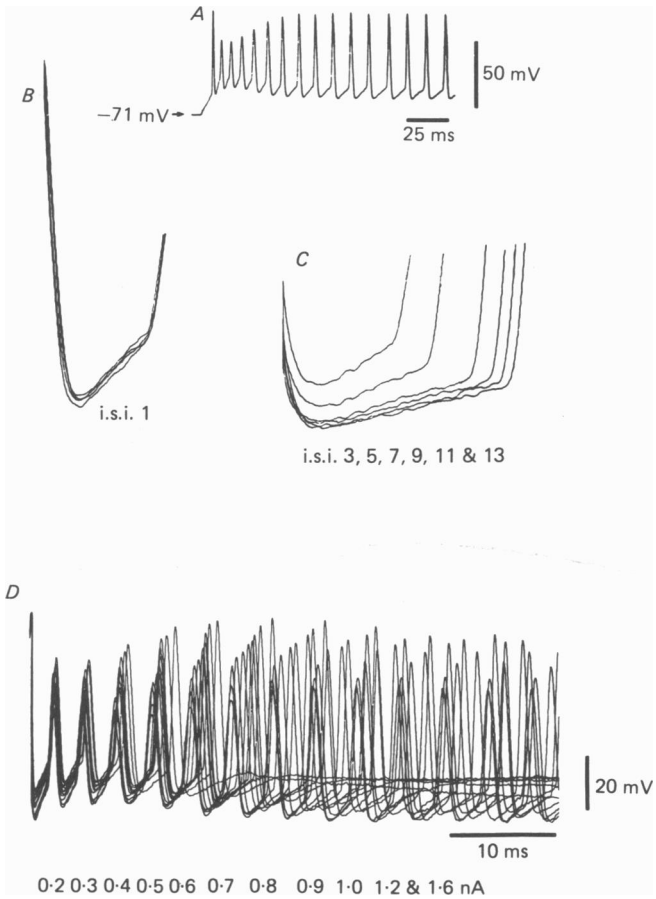

Fig. 10. Repetitive firing of thalamic neurone produced by intracellular injection of outward current pulse. *A*, response to injection of 0·8 nA. The initial burst is immediately followed by a train of action potentials reaching a constant amplitude and followed by a.h.p.s of constant size and duration. *B*, the first interspike interval (i.s.i.) from four superimposed traces similar to the one shown in *A*; note the constant amplitude and duration. *C*, interspike intervals 3, 5, 7, 9, 11 and 13 taken from the record in *A*. The third a.h.p. is clearly smaller in amplitude than the first (shown in *B*) but lasts slightly longer. As the firing continues, the a.h.p.s grow in size and duration. *D*, the response of the neurone to curent pulses of increasing amplitude (0·2–1·6 nA). Note that the early firing is largely independent of the stimulus but that the late firing is deeply modulated by the amplitude of the input.

The frequency of firing was highest during the burst response, reaching a value of about 350/s for the first three spikes. During this burst the action potentials rose from higher firing levels, indicating that a certain amount of inactivation of the Na^+ conductance generating the fast spike was present, which would explain the lower amplitude and longer duration of the secondary action potentials in the burst (Fig. 10*A*). In the post-burst period the action potentials showed a rather constant amplitude and duration. They were followed by an a.h.p. whose amplitude was larger than that seen during the burst. In contrast to the increasing intervals between spikes

which occurred during the burst generation (records in Fig. 10*C*), the interspike intervals during the post-burst period were constant. The stereotyped nature of the initial potential of the burst response of the thalamic neurones at rest could be seen in Fig. 10*B* and *D*. In Fig. 10*D*, eleven superimposed traces of repetitive firing produced by current injections of increasing amplitude demonstrated a minimal degree of variability of the initial potential of the burst, especially compared to that for the action potentials which followed. If, on the other hand, the level of depolarizations was such that the initial burst was totally inactivated (due to inactivation of the l.t.s.), thalamic cells responded with a continuously graded increase of firing frequency to increasing amplitudes of depolarization.

Because of the non-linear behaviour of the repetitive firing illustrated above, the description of the frequency–current relation (*f–I* plots) in thalamic cells was particularly involved. The responses obtained in a thalamic neurone from a hyperpolarized level (−80 mV) during one-second-long square-pulse depolarizations are shown in Fig. 11. The injected currents in the three records in Fig. 11*A* differ from each other by less than 0·1 nA. It is clear, therefore, that a small modification of the amplitude of depolarization could produce a marked change in the repetitive firing of these neurones. Note in the third recording that the initial spike was followed by a silence which was itself followed by a train of spikes that gradually accommodated to a lower frequency.

The resting membrane potential from which the cell was tested also had some influence on the repetitive firing properties. Three plots are illustrated in Fig. 11*B*. In the upper left quadrant the instantaneous firing frequency at the first interspike interval after the l.t.s. was plotted against current at five different holding potentials. The frequency increased close to exponentially if the cell was depolarized from a −45 mV holding potential. By contrast a rather abrupt change in firing frequency occurred if the current pulses were imposed on a rest level of −85 mV. The change in the slope of these plots with membrane potential was, however, quite gradual for the other three levels of initial membrane potential plotted (−55, −65 and −75 mV). Similar plots were made for the second spike interval (upper right quadrant) and for the interval after 1 s square-current injection (accommodated firing). Note also that *f–I* curve after 1 s of current injection was quite similar regardless of the initial value of the resting potential. In the lower right quadrant the *f–I* relations for four different cells after 2 s current injection are demonstrated. They were all obtained from normal resting potential, which was between −60 and −64 mV.

Other electrophysiological properties

While the electrophysiological properties described above were found in most of the cells throughout this population, in two cases slightly different properties were observed (see Fig. 12). One cell was recorded in a slice containing the most caudal part of the thalamus (Fig. 12*A*) and it may indeed have been an extrathalamic neurone lying close to the third ventricle. The other cell was found in the lateral nucleus (Fig. 12*B*). Typical repetitive activation was observed when the membrane was depolarized from rest but no burst could be generated when the cells were depolarized from a hyperpolarized level. However, a non-linearity could nevertheless be seen in the initial part of the depolarization (arrow). When hyperpolarizing current

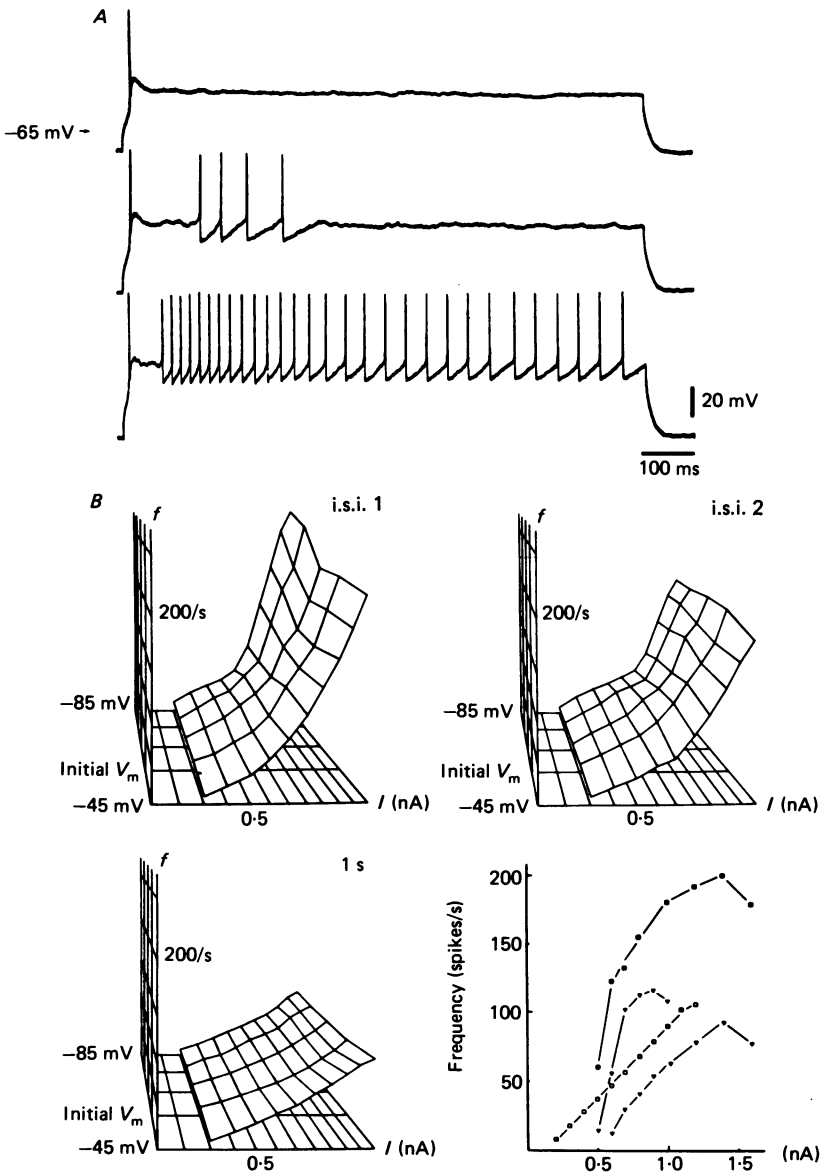

Fig. 11. Frequency *versus* injected current characteristics of thalamic neurones. *A*, response of cell to depolarizing current pulses of increasing amplitude (0·50, 0·55 and 0·60 nA). All stimuli produced an early burst response and the two larger stimuli elicited repetitive firing after the burst. Upper left *B* shows the instantaneous frequency at the first interspike intervals in the spike train after the burst as a function of total injected current (x axis) and initial holding potential (y axis) at values of −45, −55, −65, −75 and −85 mV. A similar plot for the second interspike interval is shown in upper right *B* and a plot of the instantaneous frequency after one second is shown in lower left *B*. Only the instantaneous frequency at the first interspike interval is modulated by the initial holding potential, the frequency being higher for large currents after more negative values of the initial potential. The firing rapidly adapts to an almost linear function of injected current. Steady state (t = 2 s) f–I plots for four different cells are shown in lower right part of *B*.

pulses were delivered from rest, no burst response was seen at their break (Fig. 12*C*). These cells, on the other hand, did show a clear a.h.p. and, as can be seen on the right in Fig. 12*D*, demonstrated a clear facilitation as membrane potential was maintained at a depolarized level.

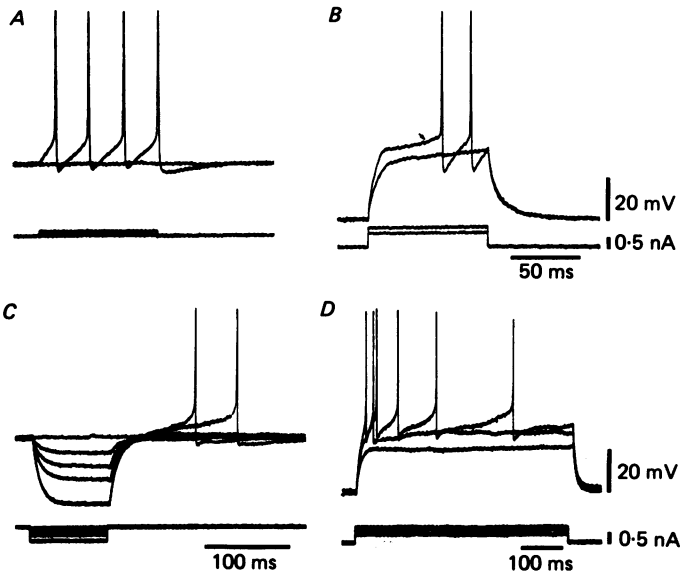

Fig. 12. Recordings from the only two cells in this study found not to have a burst response. *A* and *B*, from a cell in the caudal thalamus. Depolarization with intracellular current pulses produced fast spikes; in the case of initial hyperpolarization of the membrane the spikes were preceded by a slowly depolarizing potential (arrow in *B*). C and *D*, from a cell in the lateral nucleus showing rebound excitation (*C*) and marked after-hyperpolarizations (*C* and *D*).

DISCUSSION

The present paper described the electrophysiological properties which thalamic neurones display *in vitro*. Probably the most salient feature of our findings is the fact that neurones in the different regions of the thalamus (including 'sensory' and 'motor' regions) demonstrated very much the same electrophysiological character regardless of their particular morphology.

Four basic properties define thalamic neurones: (1) their firing is modulated by the initial membrane potential of the cell. From resting level, and especially when the cell is slightly depolarized (positive to −55 mV), thalamic neurones fire repetitively in a tonic manner when challenged with an outward current pulse, (2) if the cells have a resting negative to −60 mV and very prominently more negative than −65 mV, a single burst of spikes occurs when the cell is transiently depolarized. The burst of spikes is characterized by a very low threshold compared to the tonic repetitive firing. It has an all-or-none property, a duration of about 20–30 ms and, under normal conditions, generates one or several fast action potentials riding on the crest of a slow rising triangular depolarization, the l.t.s. These two main forms of electrical

activity characterize two functional states of the same neurone, a tonic firing property and a phasic burst response.

The other two electrophysiological properties relate to the generation of large amplitude a.h.p.s and of prolonged plateau depolarizations. The a.h.p., as demonstrated in the accompanying paper, is produced by two main mechanisms: (i) the activation of a voltage-dependent K^+ conductance, a Ca^{2+}-dependent K^+ conductance (cf. Tsien, 1983), and an early K^+ conductance, the I_A current (Connor & Stevens, 1971), and (ii) a slow return from the hyperpolarizing level to the plateau depolarization level which has a rather slow onset.

The presence of these different conductances gives thalamic neurones the ability to serve as simple relay cells or to generate burst responses and to oscillate at different stable frequencies.

Tonic firing. Thalamic cells have been reported to fire tonically and to serve as simple relay elements in several sensory and motor pathways (Poggio & Mountcastle, 1963; Jasper & Bertram, 1966). In addition, it is known that the relationship between input and firing frequency is close to linear especially for inputs of large amplitude (Mountcastle, Poggio & Werner, 1963). This type of function is clearly present in neurones maintained *in vitro* when the membrane potential is slightly depolarized (about −60 mV). The frequency during a given depolarization, however, will vary with immediate history of the membrane potential as illustrated in Fig. 11. The properties of repetitive firing are basically characterized by the presence of a non-linear relation between injected current and spike firing immediately after the onset of spike activation. This initial discharge is usually related to the presence of a partial activation of the l.t.s.

As the membrane is hyperpolarized, the l.t.s. overrides the properties of the initial spike intervals as it becomes the salient response at those membrane levels. Following this burst, the cell settles into tonic firing with a frequency related to the injected current amplitude.

The l.t.s. The amplitude of l.t.s. seems to be clearly related to the membrane potential level. The response is first observed at membrane potentials as low as −57 mV (Fig. 5*B*) as a very small all-or-none transient depolarization, indicating that the mechanism is related to a voltage-dependent conductance which is inactive at levels positive to −55 mV. As the membrane is hyperpolarized, the l.t.s. increases in amplitude and reaches a maximum at levels negative to −70 mV. The conductances underlying this response are voltage- and also time-dependent. A hyperpolarization lasting about 30 ms seems to be the minimum required to start de-inactivation of this conductance; the de-inactivation is not complete until after 170 ms. Although the l.t.s. is de-inactivated by hyperpolarization, following activation l.t.s. cannot be reactivated for 50–100 ms, even under conditions of membrane hyperpolarization. This response is in fact very similar to the l.t.s. initially described in inferior olivary neurones (Llinás & Yarom, 1981*a*) and recently encountered in spinal dorsal horn neurones *in vitro* (Murase & Randić, 1983). Similar responses to those demonstrated here have also been recently observed *in vivo* in mammalian thalamus (Deschenes, Roy & Steriade, 1982).

Another important phenomenon, which is probably quite significant in the normal physiology of the thalamus, is the l.t.s. which follows a hyperpolarizing current

injection. As such, the l.t.s. can serve as the basis for the generation of one of the thalamic oscillatory rhythms, since it generates a powerful rebound response. On the other hand, in our present experiments, which exclude the normal circuitry present in the *in vivo* thalamus, the oscillations based on this rebound potential were mainly observed following repetitive hyperpolarizing pulses or reductions of K^+ conductance by 4-AP (see accompanying paper, Jahnsen & Llinás, 1984).

The slow depolarizing potential and the after-hyperpolarization. The presence of a slow depolarizing potential is clearly evident in these neurones as shown in Fig. 8*A*. This sustained inward current allows the cells to have a continuum of 'resting' states. Indeed, a slow non-inactivating Na^+ conductance may generate a continuous plateau stage as high as 15 mV from the threshold level that can last for seconds and even minutes. The plateau potential is accompanied by an increase in membrane conductance and shortening of the membrane time constant and may reach a stable condition where the cell tends to oscillate at 9–11 cycles/s as demonstrated in the accompanying paper (Jahnsen & Llinás, 1984). The a.h.p., on the other hand, is generated by several independent K^+ conductances which include a delay rectifier (g_K), a Ca^{2+}-dependent conductance ($g_{K[Ca]}$), and the early K^+ conductance (I_A).

The present set of results describes the electroresponsiveness of thalamic neurones *in vitro*. In the accompanying paper we show the ionic basis for these properties and their relation to neuronal oscillation.

Research was supported by United States Public Health Service program grant NS-13742 from the National Institute of Neurological and Communicative Disorders and Stroke. H. Jahnsen was also supported by grants from the University of Copenhagen, the Danish Medical Research Council, the Weimann Fdn. and by an Albert Cass Traveling Fellowship.

REFERENCES

ANDERSEN, P. & SEARS, T. A. (1964). The role of inhibition in the phasing of spontaneous thalamo-cortical discharge. *J. Physiol.* **173**, 459–480.

CONNOR, J. A. & STEVENS, C. F. (1971). Voltage clamp studies of a transient outward membrane current in gastropod neural somata. *J. Physiol.* **213**, 21–30.

DESCHENES, M., ROY, J. P. & STERIADE, M. (1982). Thalamic bursting mechanism: an inward slow current revealed by membrane hyperpolarization. *Brain Res.* **239**, 289–293.

FAMIGLIETTI, E. V., JR. & PETERS, A. (1972). The synaptic glomerulus and the intrinsic neuron in the dorsal lateral geniculate nucleus of the cat. *J. comp. Neurol.* **144**, 285–334.

FRIEDLANDER, M. J., LIN, C.-S., STANFORD, L. R. & SHERMAN, S. M. (1981). Morphology of functionally identified neurones in lateral geniculate nucleus of the cat. *J. Neurophysiol.* **46**, 80–129.

GROSSMAN, A., LIEBERMAN, A. R. & WEBSTER, K. E. (1973). A Golgi study of the rat dorsal lateral geniculate nucleus. *J. comp. Neurol.* **150**, 441–466.

GUILLERY, R. W. (1966). A study of Golgi preparations from the dorsal lateral geniculate nucleus of the adult cat. *J. comp. Neurol.* **128**, 21–50.

GUSTAFSSON, B., GALVAN, M., GRAFE, P. & WIGSTRÖM, H. (1982). A transient outward current in a mammalian central neurone blocked by 4-aminopyridine. *Nature, Lond.* **299**, 252–254.

HAGIWARA, S., KUSANO, K. & SAITO, N. (1961). Membrane changes of *Onchidium* nerve cell in potassium-rich media. *J. Physiol.* **155**, 470–489.

JAHNSEN, H. & LLINÁS, R. (1982). Electrophysiological properties of guinea pig thalamic neurons studied *in vitro*. *Neurosci. Abstr.* **8**, 413.

JAHNSEN, H. & LLINÁS, R. (1984). Ionic basis for the electroresponsiveness and oscillatory properties of guinea-pig thalamic neurones *in vitro*. *J. Physiol.* **349**, 227–247.

JASPER, H. H. & BERTRAND, G. (1966). Thalamic units involved in somatic sensation and voluntary

and involuntary movements in man. In *The Thalamus*, ed. PURPURA, D. P. & YAHR, M. D., pp. 365–390. New York: Columbia University Press.

LLINÁS, R. & JAHNSEN, H. (1982). Electrophysiology of mammalian thalamic neurones *in vitro*. *Nature, Lond.* **297**, 406–408.

LLINÁS, R. & SUGIMORI, M. (1980). Electrophysiological properties of *in vitro* Purkinje cell somata in mammalian cerebellar slices. *J. Physiol.* **305**, 171–195.

LLINÁS, R. & YAROM, Y. (1981*a*). Properties and distribution of ionic conductances generating electroresponsiveness of mammalian inferior olivary neurones *in vitro*. *J. Physiol.* **315**, 569–584.

LLINÁS, R. & YAROM, Y. (1981*b*). Electrophysiology of mammalian inferior olivary neurones *in vitro*. Different types of voltage-dependent ionic conductances. *J. Physiol.* **315**, 549–567.

LUPARELLO, T. J. (1967). *Stereotaxic Atlas of the Forebrain of the Guinea Pig*. Basel: S. Karger A.G.; Baltimore: Williams & Wilkins.

MOUNTCASTLE, V. B., POGGIO, G. F. & WERNER, G. (1963). The relation of thalamic cell response to peripheral stimuli varied over an intensive continuum. *J. Neurophysiol.* **26**, 807–834.

MURASE, K. & RANDIĆ, M. (1983). Electrophysiological properties of rat spinal dorsal horn neurones *in vitro*: calcium-dependent action potentials. *J. Physiol.* **334**, 141–154.

POGGIO, G. F. & MOUNTCASTLE, V. B. (1963). The functional properties of ventrobasal thalamic neurons studied in unanesthetized monkeys. *J. Neurophysiol.* **26**, 775–806.

RALSTON, H. J., III (1979). Neuronal circuitry of the ventrobasal thalamus: the role of presynaptic dendrites. In *The Neurosciences: Fourth Study Program*, ed. SCHMITT, F. O. & WORDEN, F. G., pp. 373–379. Cambridge, MA: M.I.T. Press.

RAMÓN Y CAJAL, S. (1911). *Histologie du systeme nerveux de l'homme et des vertebres*. Paris: Maloine.

SCHEIBEL, M. E. & SCHEIBEL, A. B. (1966). Patterns of organization in specific and nonspecific thalamic fields. In *The Thalamus*, ed. PURPURA, D. P. & YAHR, M. D., pp. 13–46. New York: Columbia University Press.

SHEPHERD, G. M. (1979). *The Synaptic Organization of the Brain*. New York: Oxford University Press.

SPAĆEK, J. & LIEBERMAN, A. R. (1974). Ultrastructure and three-dimensional organization of synaptic glomeruli in the rat somatosensory thalamus. *J. Anat.* **117**, 487–516.

TINDAL, J. S. (1965). The forebrain of the guinea-pig in stereotaxic coordinates. *J. comp. Neurol.* **124**, 259–266.

TSIEN, R. W. (1983). Calcium channels in excitable cell membranes. *A. Rev. Physiol.* **45**, 341–358.

YAROM, Y., SUGIMORI, M. & LLINÁS, R. (1980). Inactivating fast potassium conductance in vagal motoneurons in guinea pigs: an *in vitro* study. *Neurosci. Abstr.* **6**, 198.

EXPLANATION OF PLATES

PLATE 1

A, reconstruction of the main nuclei in the guinea-pig thalamus; 1, medial group; 2, anteromedial; 3, anterodorsal and anteroventral; 4, lateral; 5, parafascicular; 6, ventral group; 7, lateral geniculate; 8, posterior group; and 9, rostral part of medial geniculate. Dashed lines correspond to the sections shown in Fig. 1. Numerals to the left correspond to stereotaxic coordinates (see text). *B*, 400 μm-thick slice of the guinea-pig diencephalon cut approximately at stereotaxic coronal plane 7·0 (see Fig. 1). The unstained tissue was transilluminated with a point source. Several of the thalamic nuclei are outlined to facilitate correlation with Fig. 1.

PLATE 2

Examples of thalamic neurones stained with horseradish peroxidase (*A* and *B*) and Lucifer Yellow (*C* and *D*). The large cell with a fusiform cell body in *A* was stained in the lateral nucleus and the smaller cell in *B* was located in the medial group of nuclei. In *C* is shown a large and a small cell from the ventral nucleus having overlapping dendritic fields and in *D*, an example of a ventral cell with a somewhat bipolar appearance. Its axon could be followed 300 μm from the soma (large arrow) and it sent off collaterals about 150 μm from the soma (small arrow). Calibration: 50 μm for all cells.

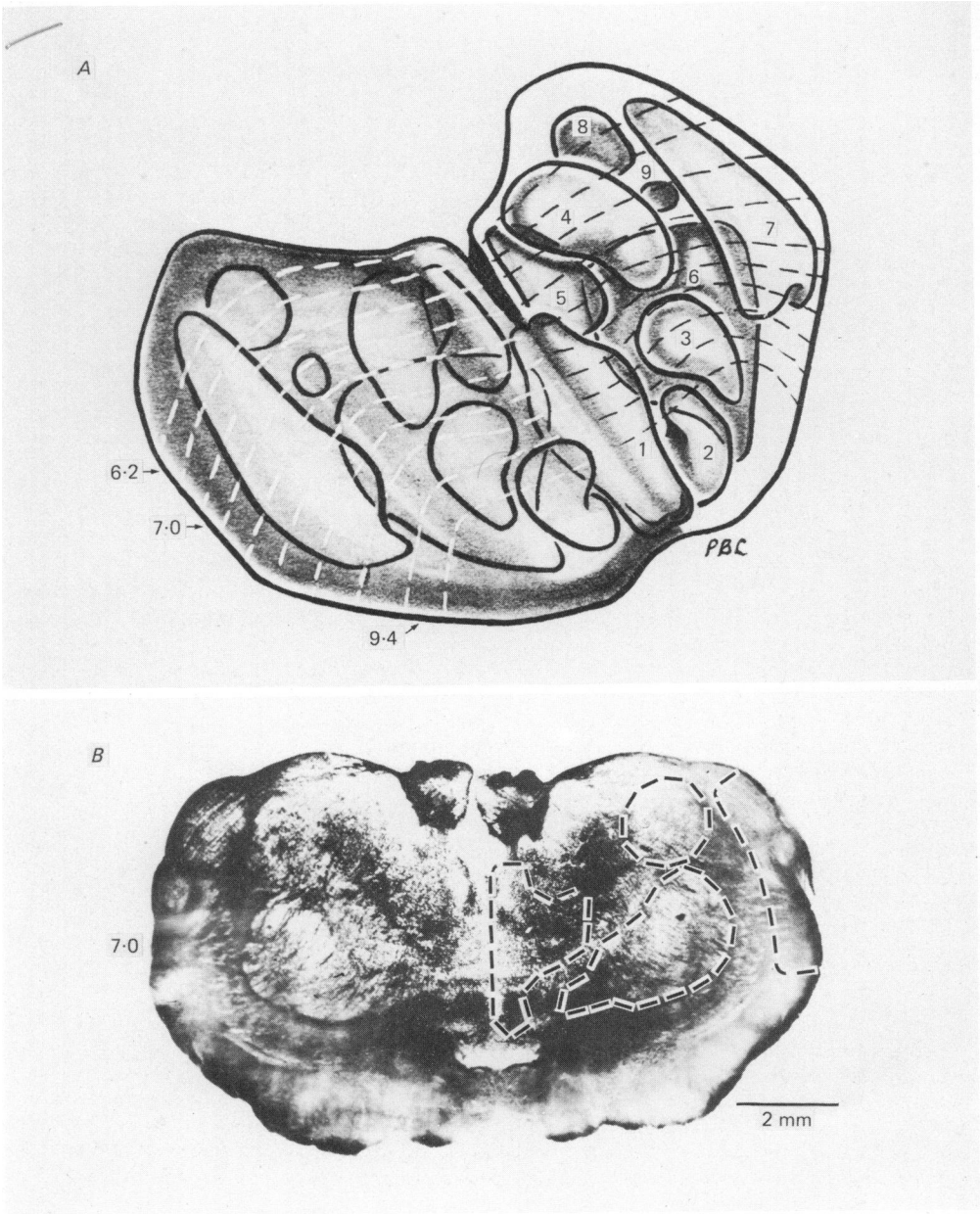
A
8
9
4
7
6
5
3
1
2
6·2
7·0
PBC
9·4
B
7·0
2 mm

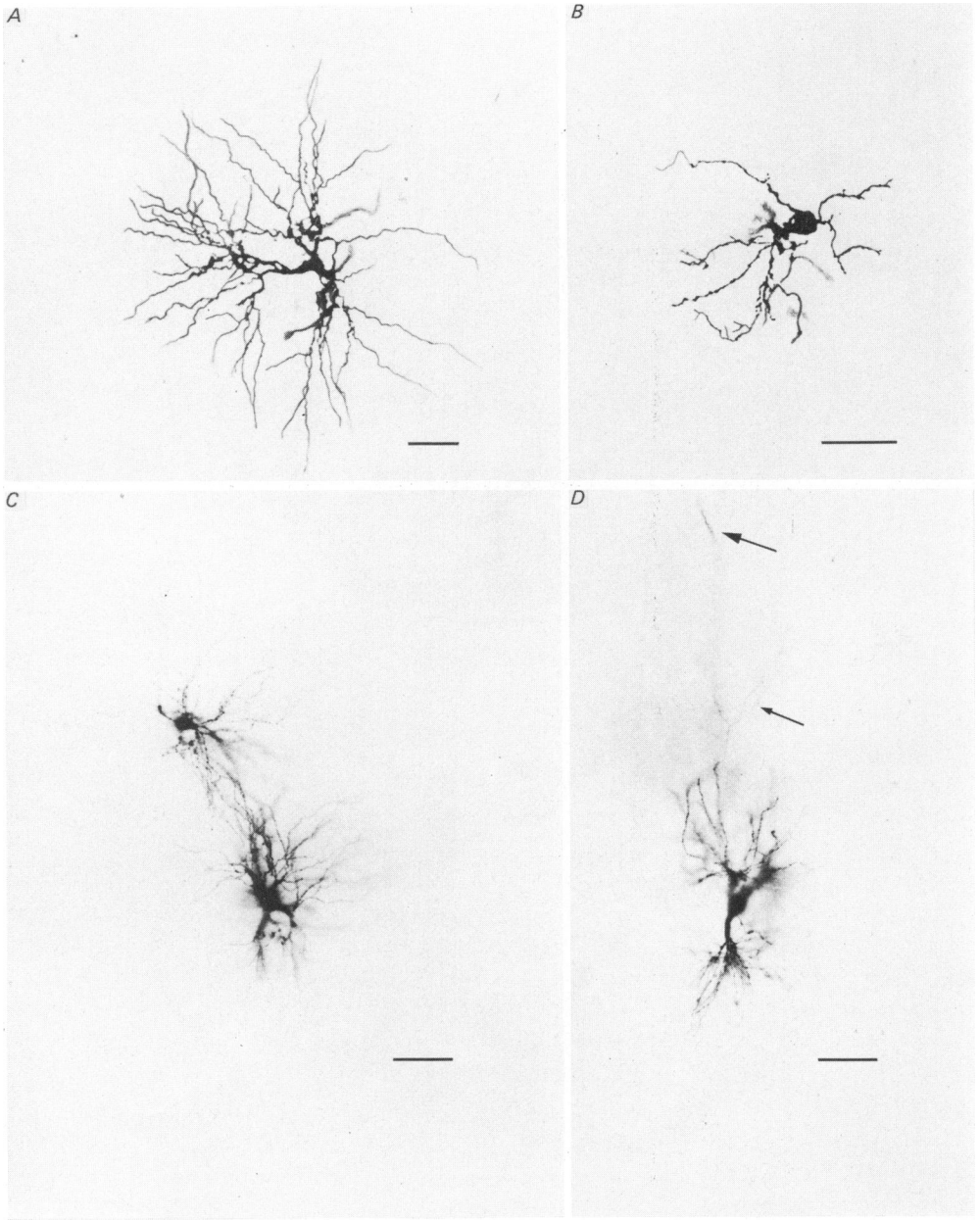
A
B
C
D